Micro Pulse Lidar

James D. Spinhirne

Abstract—**An eye safe, compact, solid state lidar for profiling atmospheric cloud and aerosol scattering has been demonstrated. The transmitter of the micro pulse lidar is a diode pumped μJ pulse energy, high repetition rate Nd:YLF laser. Eye safety is obtained through beam expansion. The receiver employs a photon counting solid state Geiger mode avalanche photodiode detector. Data acquisition is by a single card multichannel scaler. Daytime background induced quantum noise is controlled by a narrow receiver field-of-view (FOV) and a narrow bandwidth temperature controlled interference filter. Dynamic range of the signal is limited by optical geometric signal compression. Signal simulations and initial atmospheric measurements indicate that systems built on the micro pulse lidar concept are capable of detecting and profiling all significant cloud and aerosol scattering through the troposphere and into the stratosphere. The intended applications are scientific studies and environmental monitoring which require full time, unattended measurements of the cloud and aerosol height structure.**

I. Introduction

LIDAR has been a research tool for over 20 years. However, even though there are significant potential applications, routine operational use of lidar, in the mode common for radar, has not happened. There are three primary limitations which have held back the use of current conventional lidar systems. The first factor is the lack of eye safety of pulsed laser transmitters for ground personnel and aircraft operations. Safety considerations oblige that systems require constant supervision whenever non eye safe laser beams are in use. A second limitation is the cost, size, and complexity of the lidar systems that are now employed for atmospheric research. Third, although the technology is rapidly advancing, the lack of reliability of the conventional pulsed laser has been a problems for routine lidar use. The effect of the second and third, and also the first, factors given above is that lidar use is personnel intensive. For routine or full time lidar observations for applied or scientific applications, eye safe, turn key, autonomous systems are what are needed.

Recent advances in technology make possible what we believe can be considered a new type of laser radar system which is eye safe, simple, low cost and capable of full time unattended aerosol and molecular scattering observations. Conventional visible wavelength lidar systems which have been employed for most published lidar work to date make use of 0.1 to 1.0 J class lasers and operate at pulse repetition rate of up to several tens of Hertz [1]. The basic concept of the lidar that we will describe here is a system with micro Joule level pulse energies and pulse repetition rates of several thousand Hertz and which in addition employs efficient photon counting signal detection and acquisition. The low pulse energy permits transmitted beam energy densities that are within eye viewing safety standards. With micro Joule pulse energies the return signal levels for aerosol and molecular observations are within the range where quantum noise limited photon counting detection is necessary. Technologies which now make the lidar practical are small diode pumped Nd:YAG and Nd:YLF lasers, solid state Geiger Avalanche Photo Diode (APD) photon counting detectors and single card, low cost multichannel scalar signal acquisition. Since the components are all solid state good reliability is to be expected. In this paper we will present a discussion of the applications, potential and limitations for micro pulse lidar (MPL) and also present results from an initial breadboard prototype system.

Manuscript received April 15, 1992; revised July 1, 1992. This work was supported by the Goddard Space Flight Centers Directors Discretionary Fund.

The author is with the Laboratory for Atmospheres/917, Goddard Space Flight Center, Greenbelt, MD 20771.

IEEE Log Number 9204841.

II. MPL Concept and Applications

The two most basic parameters which determine the performance of a lidar system are the transmitter power and the receiver aperture. Twenty years ago this author employed a lidar system with a 0.2 m receiver and a ruby laser that could transmit a 1 J pulse three times a minute or 0.05 w transmitted power. The system was more than adequate for aerosol scattering measurements in the cleanest air conditions throughout the troposphere and beyond [2]. Diode pumped Nd:YAG and Nd:YLF lasers with pulse energies in the ten's of micro Joules and PRF (Pulse Repetition Frequency) beyond 10 kHz are now commercially available. Pulse repetition rates for lidar of up to 3 to 10 kHz are possible before interference between signals from consecutive pulses is a limit. For 10 μJ pulses 0.05 w is transmitted at 5 kHz PRF. A MPL system with a 0.2 m aperture and an appropriate design should in principal then be adequate for clear air observations. However, for low pulse energies, detector efficiency and noise, and especially background signal noise, is a much more significant problem than for a high pulse energy system. As will be discussed below the detector and background problems are manageable.

Eye Safety: Our goal for an eye safe lidar is a transmitted beam that is safe at all ranges including at the exit aperture. For pulse energy in the micro Joule range eye safe power densities may be obtained by sufficiently expanding the transmitted beam. For the ANSI Z136.1-1986 laser exposure safety standard [3] the maximum permissible exposure (MPE) is 5×10^{-7} J/cm^2 in the 520–530 nm wavelength range. In addition the MPE must be reduced by a factor of $N^{-.25}$ for repetitive pulses where N is the number of pulses incident on the eye. For visible light it is assumed that the natural aversion response will limit exposure to 0.25 s, or 1250 pulses at 5kHz PRF. The

permissible energy density in that case is 8.4×10^{-8} J/cm^2. For a laser beam expanded to 0.2 m diameter a 25 uJ pulse energy is within the eye safety limit for direct viewing. Limits for other pulse energies are readily calculated, 40 μJ for 25 cm and 4 μJ for 8 cm. Other factors for the eye safety of a laser transmitter are eye aided viewing and scintillation [4]. Eye-aided viewing is not considered a factor for upward directed beams. Scintillation involves focussing of the laser beam due to turbulence-induced refractive index fluctuations in the atmosphere and is more of a consideration for horizontal than vertical beams. An additional margin for scintillation could be necessary, but in the far range a margin arises from beam expansion and atmospheric attenuation. It may also be noted that the Federal Aviation Administration limits for transmitted radiation are much higher than the ANSI standard. The pulse energy needed for an MPL transmitter may thus be obtained with eye safety by reasonable expansion of the beam.

Signal Detection, Background and Dynamic Range: As will be given below, signals for an MPL system will be in range of a few photons per microsecond or less. At such signal levels quantum noise limited detection is required, and in practice photon counting signal acquisition is needed. Photon counting signal detection has been previously applied for lidar receivers, typically for high altitude measurements [5]. The systems have employed photo-multiplier (PMT) detectors with discriminators and multichannel scalers for the signal acquisition. The systems are bulky, require high voltage and the quantum efficiency is typically 5–20%. Solid sate detectors were formerly too noise rich for quantum limited detection. This changed with the recent development of solid state, Geiger mode Avalanche Photo Diode (GAPD) detectors for photon counting signal detection [6]. They are available packaged in a small self contained module with a pre-amp and discriminator. A very significant advantage is high quantum efficiency, over 40% in the 520 to 530 nm wavelength region. Although a MPL system could employ PMT detection, the GAPD detector provides a very major, almost enabling, performance and design improvement. GAPD's which would be usable in the one micron wavelength region of the Nd:YLF and Nd:YAG fundamental wavelengths are not now available. As discussed later, a one micron wavelength GAPD if available could significantly improve MPL system design.

At small signal levels, quantum noise from background sky radiance is the limiting factor for daytime lidar measurements and will be a significant problem for an MPL system. Two approaches can be taken to limit background signals in a lidar receiver relative to the backscatter return signal, reducing the receiver wavelength bandwidth and reducing the receiver field-of-view (FOV). Both approaches are required for an MPL system.

A limitation of low PRF photon counting lidar receivers has been the dynamic range of the signal acquisition. If n_r is the maximum linear count rate, typically less than 10 counts/μs, then to acquire a signal of Q reduced magnitude at the same signal to noise as an unsaturated n_r signal requires summing over Q^2 times as many pulses. A dynamic range of two orders of magnitude will require averaging over 10^5 to 10^6 pulses; this is compatible with, and an advantage of, the MPL approach. However the backscatter cross section for the full range of atmospheric scattering varies by over four orders of magnitude, and range squared signal dependence can add another three to four orders of magnitude to the dynamic range of a lidar signal. Dynamic range compensation in addition to pulse summation is required for a photon counting lidar system if a temporal resolution on the order of seconds is required and the photon counting rate is limited. A very significant dynamic range compression can be obtained through geometric signal compression [7]. Geometric compression is obtained by optics design and is compatible with the small FOV requirement mentioned above. Depending on the application, additional active optical compression may be required.

System Comparison: Two previous types of laser radar foreshadow the type of system we are describing. Laser diode ceilometers which are commercially available and widely used are in fact solid state, eye safe, autonomous laser radar instruments. However, their performance is limited. Even cloud detection is limited to 3 to 7 km, and the ceilometers do not reliably detect cirrus. A study has been made of the application of diode ceilometers to profile boundary layer aerosols [8]. The results were generally unfavorable. Whether the performance of diode ceilometers may be significantly enhanced over current instruments is beyond our scope here.

A high PRF lidar with photon counting data acquisition is the University of Wisconsin High Spectral Resolution Lidar (HSRL) [9], [10]. In concept, the HSRL is similar to the MPL. However, the HSRL was intended for a specific complex measurement which involves spectral separation of the molecular and aerosol backscatter return. An original HSRL was based on a CuCl laser and employed complex etalon filters and PMT detectors. Our current emphasis for MPL is as a simple general purpose elastics scattering lidar for cloud and aerosol applications.

Another approach for eye safe lidar is to operate at near infrared wavelengths which are beyond the transmission range of the eye's cornea. We have employed in a recent aerosol backscatter experiment a lidar system which operated at the eye safe wavelength of 1.54 μm [11]. However, at present incoherent near infrared lidars are severely limited in performance by the noise level of available detectors. A large high power liar is required to obtain aerosol measurements. Near infrared lidars which employ coherent signal detection [12] have much potential but are complex and will likely remain sophisticated and expensive instruments.

Applications: Potential applications for MPL systems are both for scientific use and applied environmental monitoring. Observation of cloud base height and profiling cirrus is important for surface radiation budget and climate modelling in general [13]. Current ceilometer instruments are not adequate for the cloud radiation applications. Routine lidar measurements to study the interaction of clouds and aerosols with the atmosphere have been attempted or are ongoing. A number of organized scientific projects in the area of clouds and atmospheric radiation have required, or emphasized, high quality lidar cloud profiling. These include ECLIPS (Experimental Cloud Lidar Pilot Study) [14], ISCCP (International Satellite Cloud Climatology) regional experiments [15] and the

ARM (Atmospheric Radiation Measurement) Program. Some programs have involved intensive use of research quality atmospheric lidars. The future points toward a requirement for long-term measurements at an increasing number of sites.

Lidar is possibly the best tool for ground-based measurements of the atmospheric aerosol loading and structure. Monitoring of the stratospheric aerosol layer by lidar has been a long term endeavor at a number of sites around the world [16]. Tropospheric aerosol structure and in particular planetary boundary layer, or inversion, height measurements by lidar have been employed increasingly in atmospheric field experiments for atmospheric dynamics, pollution and other studies. These measurements could be potentially obtained more simply and routinely by a MPL type lidar.

Applied environmental observations that could be potentially improved by MPL instruments would be improved cloud ceilometry and visibility monitoring. An application that would possibly be enabled would be monitoring of haze optical thickness, visibility and inversion heights for pollution level modeling and prediction.

III. Performance Simulations

The performance of MPL systems has been simulated. The analysis requires a signal equation, a model for atmospheric scattering and instrument system parameters. These are described below.

Signal Equation: The equation for the lidar return signal in terms of photo electrons per time n may be given as

$$n(r) = cE(r)A_rT_oQ_eJ(\beta_m(r) + \beta_p(r))T^2(r)/2qr^2 \quad (1)$$

where r is range, E is the transmitter receiver geometric overlap factor, A_r is the receiver area, T_o is the system optical transmission, Q_e is the detector quantum efficiency, J the transmitted pulse energy, β_m and β_p the molecular and particulate backscatter cross section, q the photon energy, and T the atmospheric transmission.

In addition to the backscatter signal, the lidar detector signal will include any contribution from background photons n_b given as

$$n_b = I(\lambda)A_rT_o\Omega\Delta\lambda Q_e/q \quad (2)$$

where $I(\lambda)$ is the background intensity, Ω the receiver FOV solid angle, and $\Delta\lambda$ the receiver optical bandwidth.

The lidar equation (1) includes the geometric overlap factor $E(r)$. $E(r)$ is equal to 1.0 at far ranges. At short ranges $E(r)$ is less than 1.0 and accounts for the fact that the telescope aperture of a lidar receiver is normally not the limiting aperture stop for the receiver optics for signals from short ranges. The sketch in Fig. 1 indicates the outer profile of the receiver and transmitter FOV for a bi-axial lidar design. The range where the lines labeled a and b intersect would be the range for the laser pulse to be fully in the receiver FOV for all elements of the receiver aperture. The overlap range is where $E(r) = 1.0$ initially and is given by $r_v = 2d/(\Theta - \alpha)$ where Θ and α are the transmitter and receiver full FOV angles, respectively, and d is the maximum separation of the

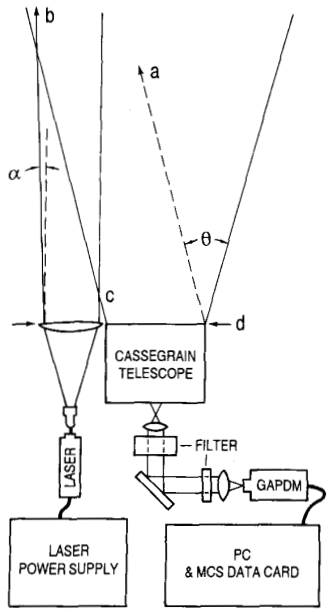

Fig. 1. A basic diagram of the micro pulse lidar breadboard system. A diode pumped Nd:YLF laser is expanded and collimated by a microscope objective and condensing lens combination. The signal collected by the Cassegrain receiver telescope is collimated through narrow bandwidth interference filters and focused on to the Geiger avalanche photodiode detector. The photon counting signal from the GAPD module is acquired by a PC computer with a multichannel scaler interface card. The transmitter FOV is shown as α and the receiver FOV is θ. At the range c the initial signal is received. At the range where the lines a and b intersect the backscattered signal is fully in the receiver FOV.

transmitter-receiver apertures. For results to follow $E(r < r_v)$ is calculated by numerical integration using equations such as given by Harms [7] and earlier references. The equations and numerical integration include the effect of the defocused image of the laser backscatter region in the receiver field stop for ranges not equal to the receiver overlap range. As mentioned previously the $E(r)$ factor can be designed for beneficial geometric compression of the dynamic range of the lidar return signal.

Atmospheric Model: For remote sensing simulations we have developed an analytic model of a vertical profile for atmospheric aerosol scattering. The model is based on extensive aerosol lidar measurements by the author and others [2] [1]. The vertical distribution for the smooth background component of the aerosol scattering is given by

$$\sigma(h) = \sigma_o(1+a)^2\exp(h/b)/[a+\exp(h/b)]^2 + f(1+a')^2\exp(h/b')/[a+\exp(h/b')]^2 \quad (3)$$

where $\sigma(h)$ is the aerosol extinction coefficient at altitude h. The terms σ_o, a, a', b, b', f are constants. For the current model $\sigma_o = .025$ km^{-1}, $a = .4$, $a' = 2981$, $b = 1.6$ km, $b' = 2.5$ km and $f = 1.5e{-}7$ km^{-1}. The background particulate backscatter cross section is then $\beta = \sigma/S_p$ where S_p is here chosen to be a constant value 30 sr as representative of tropospheric aerosols [17]. In addition to the smooth aerosol model above,

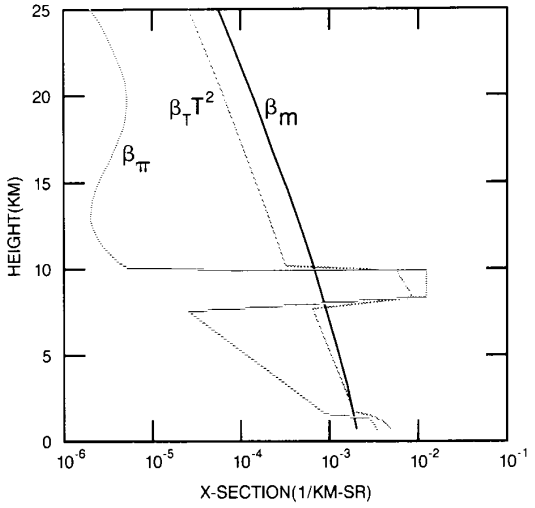

Fig. 2. An atmospheric model is employed to simulate the performance of lidar instruments. The particulate backscattering value β_p is the sum of an analytic smooth background aerosol profile plus cirrus and boundary layer aerosol scattering layers. The molecular backscatter cross section β_m is calculated for 523 nm wavelength. The term $\beta_t T^2$ includes the total backscatter cross section and atmospheric transmission and is the atmospheric term in the lidar signal equation.

a discontinuous boundary layer aerosol scattering increase is added to the model. For the boundary layer, $\sigma(h) = \sigma(h) + 0.05$ km^{-1} for h from 0 to 1 km altitude.

Cirrus cloud profiling will be the most difficult cloud measurement for ground based lidar, and a cirrus layer is added to the model. For the cirrus layer $\sigma_c = 0.1$ km^{-1} is used and the layer extends from 8.0 to 10.0 km. The cirrus backscatter is $\beta_c = \sigma_c / S'_c$ where $S'_c = 10.0$ sr [18] is applied as the effective extinction to backscatter ratio.

The overall particulate backscatter cross section $\beta_p(h)$ for the atmospheric scattering model is shown in Fig. 2. The molecular backscatter cross section β_m for the Nd:YLF II wavelength of 523 nm is also shown and is calculated for the US Standard Atmosphere mid latitude model. The lidar backscatter is a function of the atmospheric quantity $\beta_t T^2$ which is also shown in Fig. 1 where β_t is the sum of all scattering and the transmission T is determined from the integral of the model's total extinction cross section. The aerosol scattering profile is based on older measurements, but it may be noted that the model is consistent with measurements from the recent Global Backscatter Experiment [11]. The value for β_c, 0.01 (km-sr)$^{-1}$, is consistent with a median value from extensive cirrus observations by an airborne cloud lidar system [18]. The model includes an increase in scattering for a background statospheric aerosol layer with the peak at 20 km altitude and a particulate to molecular scattering ratio there of 5%.

System Parameters: System performance for three sets of MPL instrument parameters is presented. The parameters are listed in Table I. In the analysis a Nd:YLF laser with a 523 nm wavelength was assumed for all three systems. In keeping with the goal of compact instruments, the largest receiver aperture

TABLE I
SYSTEM PARAMETERS

System	1	2	3
Pulse Energy (uJ)	2	10	25
Receiver Diameter (m)	0.075	0.2	0.2
Optical Transmission	0.08	0.1	0.2
Detection Quantum Efficiency	0.3	0.4	0.4
Receiver Full FOV (urad)	100	100	100
Transmitter Full FOV (urad)	80	50	50
Filter Bandwidth (nm)	0.2	0.2	0.2
Day Background Signal $I(\lambda) = 0.34 F_s/\pi$ $(P_e/\mu s)$	0.06	1.0	2.1

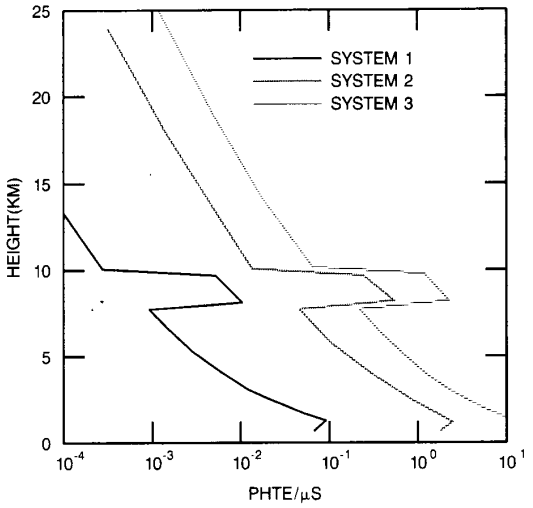

Fig. 3. The calculated received signal in photoelectrons detected per μs for three possible MPL systems as based on the model atmosphere and the system parameters given in Table I.

was assumed as 0.2 m. The first system is considered as an instrument with minimal size, power, and optical component quality. This is reflected by the 7.5 cm aperture, 2 μJ pulse energy, and .08 optical transmission. The second system would be representative of an instrument based on a laser with a 1 W diode pump, a 0.2 m aperture and nominal optic transmission. The third system would reflect optimal parameters for a 0.2 m receiver and transmitter at our stated 25 μJ eye safe pulse energy limit. The overlap range r_v was approximately 4 km for all the model systems.

Signal Simulation Results: The calculated signals $n(r)$ for each set of system parameters and our applied atmospheric model are shown in Fig. 3. For the small system 1, signals are below 0.1 P_e/μs for all ranges. The signals for system 2 exceed 1 P_e/μs in the lowest few kilometers and would then be beyond the effective linear range of the current GAPD detectors. Signals for system 3 are beyond the 1 P_e/μs range for the lowest 5 km and in the cirrus layer. Signals would still be in range for PMT photon counting. A technique to compress the signal acquisition dynamic range further than geometric compression is possible. One could sequentially increase T_o for the system between successive groups of pulses in order to acquire the out of range signal components, for example.

In the daytime the background photon rate n_b will be added to the laser signal. Values of n_b are given in the last row of Table I for an assumed background of 0.2 w/m^2-sr-nm [20], a value which would be near the upper level for a bright clear sky or thin cirrus background. It would correspond to one third the solar Lambertion diffuse intensity F_s/π where F_s is the directly transmitted solar irradiance. The background signal must be subtracted in order to obtain the backscattered lidar signal. In practice the background can be found from averages over a backscatter signal dead time at the end of each pulse return. The requirement to measure n_b lowers the possible system PRF.

Calculations of the signal-to-noise ratio (S/N) of the three systems are shown in Fig. 4. The signal-to-noise ratio is determined as

$$S/N(r) = n(r)\Delta t/[(n(r) + n_b)\Delta t]^{\frac{1}{2}} \quad (4)$$

where Δt is time bin for the signal acquisition. For the calculations of S/N given here, $\Delta t = 0.5$ μs. An additional term can be included in (4) to account for the error in background signal subtraction [21]. If the dead time mentioned above is sufficient however the additional error will be small. The results in Fig. 4 are for a sum of 10^4 pulses. For an MPL system, that would be equivalent to several seconds of signal counting for each signal return. The S/N for a day time and night case for each system are shown in Fig. 4. The day time case background photoelectron rate is that given in the last row of Table I. The background induced quantum noise significantly decreases S/N. Also it may be seen that these maximum expected background count rates for the 0.2 m systems are beyond the level for linear operation for the current GAPD detectors. A corrective measure would be to increase the system optical transmission T_o for daytime measurements, although the S/N would also then be decreased. A system with light divided among several GAPD detectors would also be possible.

From the signal analysis above it may be seen that all three systems could be applied for tropospheric aerosol and cirrus profiling. Although for the small system, signal integration times longer than a few seconds would be required, and in the day time, a signal average over several minutes would be required to profile cirrus and boundary layer aerosols with better than 10% S/N limited accuracy. This is quite adequate for many applications. System 2 with a 0.2 m aperture and 10 μJ transmitter would adequately profile cirrus and boundary layer aerosol in several seconds, day or night, and even in day time produce a full scattering profile to the molecular level for the troposphere in several minutes.

The most difficult of the proposed applications mentioned previously would be profiling statospheric aerosols. Under background aerosol loading of the stratosphere, signal accuracy of 1% or better would be required to resolve aerosol scattering from the molecular signal. For system 3 the measurement could be obtained at night with signals summed over several hours. At 300 m vertical resolution, which would be adequate, S/N would be twice that shown in Fig. 4. For a strong volcanic eruption cloud such as the current cloud from Pinatubo [19], a few minutes averaging would be sufficient.

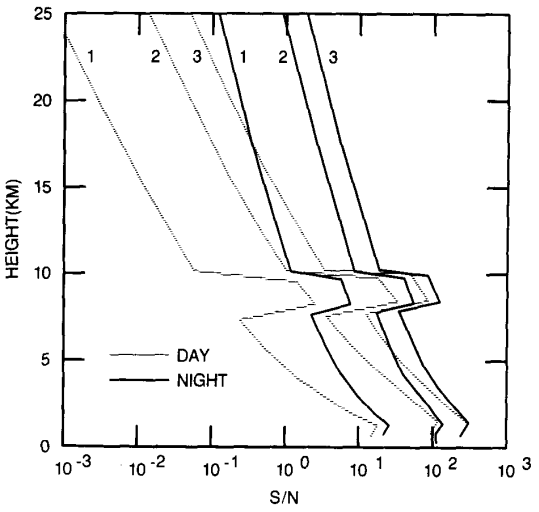

Fig. 4. The calculated signal-to-noise ratio (SNR) for the signal of the three sets of system parameters given in Table I and for the model atmosphere. The calculation assumes a summation over 10^4 pulses, or 2 s at a 5 kHz PRF, and 75 m vertical sampling. The curves for night assume no background signal noise. For the day case a background of one third the diffuse solar Lambertion intensity is applied which would be near the maximum value expected for the zenith sky.

For the stratospheric layer, a single profile per night would serve basic requirements for long term monitoring. An MPL system could not replace the large lidars which are employed for high spatial and temporal resolution measurements of the stratosphere, but limited stratospheric aerosol measurements should be a feasible application for an MPL system with a 0.2 m receiver. A 0.3 m and 40 μJ system would be four times more effective and should be possible.

A technology advancement that could significantly enhance the potential of MPL type systems would be the development of solid state quantum noise limited detectors in the 1 μm wavelength region. Eye safe power densities are approximately an order of magnitude larger at 1 μm than for 0.5 μm, and a near infrared laser beam would be invisible. Also the molecular scattering signal is reduced by a factor of 16, enhancing the discrimination of aerosol scattering. The development of these detectors has already been suggested as feasible [6].

IV. Breadboard MPL

An MPL system has been assembled and tested as a breadboard optical assembly. The basic system configuration is as shown in Fig. 1, and Fig. 5 is a picture of the assembly. The transmitter and receiver are bi-axial. The laser is a Spectra-Physics model 7300 Nd:YLF system with the beam expanded and collimated by a simple microscope objective and condenser lens combination to 8 cm diameter. The receiver telescope is a surplus, custom designed F3, 0.2 m diameter Cassegrain system. In order to employ available parts, a simple, nonoptimal, optics design was used for the breadboard receiver. Two lenses collimate the receiver beam through a narrow band filter and also image the detector at the telescope focal plane. The detector is thus the field stop. For the RCA SPCM-100-PQ GAPD detector module, the highest detection

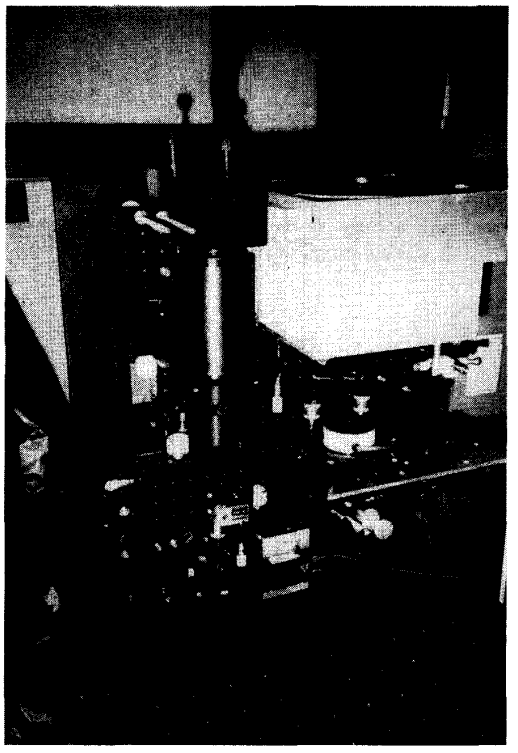

Fig. 5. A photograph of the MPL breadboard test system.

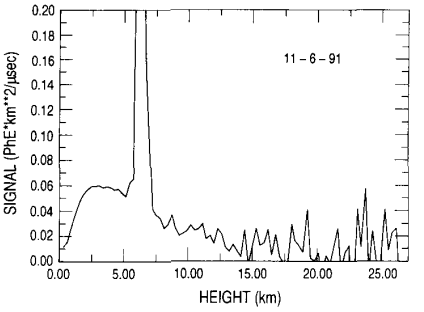

Fig. 6 A received atmospheric signal from the MPL breadboard system. The profile is a 30-min average that was acquired at sunset on November 6, 1991. The signal increases from zero to 4 k as the pulse comes into the full receiver aperture FOV. At 6 k altitude a thin cloud layer was present and produced a signal beyond the plotted range. Above the cloud layer the signal fluctuations would be due primarily to signal quantum noise.

efficiency is in a 50 micron center radius, dropping in half at 75 microns. The FOV response was thus not sharply defined. The first interference filter had a 0.25 nm bandpass and was temperature controlled for stability. A second 3 nm filter was used in the breadboard only for mechanical ease of sealing the detector from stray light. A mirror with fine control optic mounts was used for detector alignment.

A difficulty with a small FOV photon counting lidar is the alignment, or boresite, of the transmitter beam and receiver FOV. A precision corner cube retro-reflector was used for the initial alignment and the final boresite was accomplished by centering on far range cloud signals. For small FOV, scintillation, or thermal beam wandering, is a possible problem for the boresite stability. However receiver–transmitter alignment instability due to scintillation has not been observed to be a problem.

The MPL data system is simple and low cost. It consist of a 386 PC computer with a Santa Fe Energy Research Nucleus Multichannel Scaler Card (MCS-II). The range bin of the current MCS is 2 μs although 1 μs is available. The GAPD detector module output may be fed directly to the MSC. The lidar return signals from multiple pulses are internally summed by the MSC and may be read out at any programmed interval. The current system features real time, height–time–intensity display of the signal data on the PC display screen.

Results: The performance of the breadboard system was expected to be similar to system 1 simulated earlier with a 0.075 m aperture. Although the breadboard telescope aperture is 0.2 m, the overall optical transmission in less than 1.0% due to the second interference filter and uncoated optics. In addition the blur circle of the available Cassegrain telescope was 0.09 mrad, and as a result the effective detector quantum efficiency for the returned laser signal is less than 30%.

Examples of signals from the MPL breadboard system are shown in Figs. 6 and 7. The profile in Fig. 6 is an average over approximately 30 minutes with the laser operating at 2.5 kHz PRF. At the given PRF there is a 60 km range equivalent time interval between laser pulses. The last one half of the time interval was applied as the dead time by which the background count rate signal was determined. The background averaged over 10-s intervals were subtracted from the total counts to obtain the signals which were averaged for the profile shown. The data were acquired on November 6, 1991 at the time of sunset. For the measurement example, a thin, broken cloud was at 6 km. The data are displayed multiplied by the range squared with the background count level subtracted. The cloud signal is beyond the plot range but was not saturated. The overlap range of the breadboard system was approximately 4 km. No correction below that distance is shown in Fig. 6 for the fall-off of the signal due to the near range optical factor. The signal above the cloud was obtained both between and through cloud cells. Above 10 km the signal fluctuations are due primarily to signal photon shot noise. The increased signal at 22–27 km is consistent with the altitude of the strong stratospheric volcanic aerosol layer [19] that was present at the time the data were acquired.

A time height display of MPL data for another case is shown in Fig. 7. A thin cloud layer was observed over a 8-hour time period. The sun set at two hours into the data sequence. The cloud layer could be seen visually but was also sufficiently thin that background stars and sky could be seen through the layer. The thin cloud layer is seen to be clearly defined by the MPL data. Our current experience with the MPL breadboard system is that all visually apparent clouds including cirrus can be profiled with signal averages of a few minutes. For the given low optical transmission and poor detector coupling of the breadboard design, the MPL signal magnitudes are in the range that would be expected.

We are currently constructing an MPL instrument with diffraction limited, coated optical and a high transmission nar-

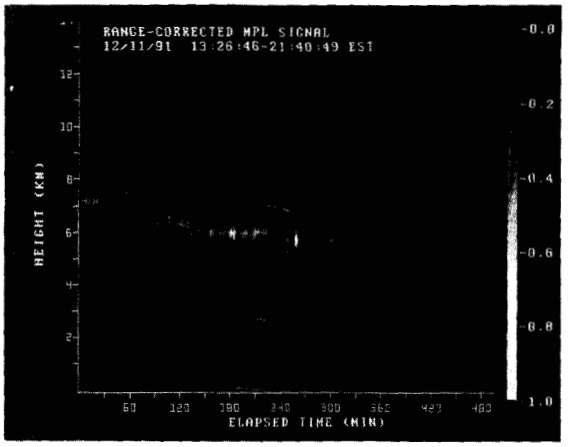

Fig. 7. An 8-hour observation of a thin cloud layer. The grey scale is proportional to the signal strength. The sun set at approximately 2 hours into the data record. The cloud layer was visually apparent but was sufficiently optically thin that sky and stars could be seen through the layer.

row band filter. The receiver optics design is such that the FOV is defined by a fixed stop and the primary mirror is imaged onto the detector to provide a well defined FOV and good detector efficiency. The receiver is 0.2 m, and the performance is expected to be that given for system 2 simulated earlier. Factors which will require operational development and testing are the correction for the overlap factor $E(r)$ and dynamic range compensation. The design is intended to be sufficiently stable that drift in alignment will not be a factor that will cause $E(R)$ to vary. The application of the system will be for cloud and aerosol height profiling in atmospheric radiation field experiments and monitoring programs.

V. Summary

The micro pulse lidar goal is an eye safe instrument for profiling clouds and aerosol structure throughout the atmosphere. Eye safety is obtained by transmitting low power pulses in an expanded beam. In order to achieve good measurement sensitivity the laser transmitter is operated at high PRF, and signals are acquired through high efficiency photon counting. Small receiver FOV and optical bandwidth serve to limit background induced noise for daytime measurements. The components on which our MPL design is based are diode pumped Nd:YLF lasers, GAPD photon counting detectors and single card multichannel scalar data acquisition. Signal simulations and initial measurement results show that it is possible to construct compact, all solid state lidars of the MLP type which have the performance to monitor all cloud and significant aerosol scattering throughout the troposphere and into the stratosphere. The proposed uses are scientific studies and environmental monitoring applications which require full time, unattended measurements of the cloud and aerosol height structure. With further development, the MPL[1] concept has a potential to become a significant instrument technology for environmental remote sensing.

[1]Another name that has been suggested to differentiate the design from conventional lidar is "phodar" since the detection and ranging is fundamentally in a photon mode. A review of published literature over the last 20 years indicates no previous reference to the term.

Acknowledgment

The work reported in this paper would not have been accomplished without the assistance of Mr. Vibart S. Scott for assembly and testing of the breadboard instrument and of Mr. Luis A. Ramos-Izquierdo for optics.

References

[1] J. A. Reagan *et al.*, "Lidar sensing of aerosols and clouds in troposphere and stratosphere," *Proc. IEEE,* vol. 77, pp. 433–448, 1989.
[2] J. D. Spinhirne *et al.*, "Vertical distribution of aerosol extinction cross section and inference of aerosol imaginary index in the troposphere by lidar technique," *J. Appl. Meteor.*, vol. 19, pp. 426–438, 1980.
[3] American National Standards Institute, "American national standard for the safe use of lasers," ANSI Z136.1-1986, pp. 1–96, 1986.
[4] W. F. Dabberdt and W. B. Johnson, "Atmospheric effects upon laser eye safety-Part II," Stanford Research Institute tech. document, pp. 1–92, 1971.
[5] S. K. Poultney, "Single photon detection and timing: experiments and techniques," *Adv. in Elctr. and Elct. Phys.,* vol. 31, pp. 39–117, 1972.
[6] A. W. Lightstone and R. J. McIntyre, "Photon counting silicon avalanche photodiodes for photon correlation spectroscopy," *Proc. of the OSA Topical Meeting on Photon Correlation Techniques and Applications,* (Washington, DC), pp. 183–191, 1988.
[7] J. Harms, "Lidar return signals for coaxial and noncoaxial systems with central obstruction," *Appl. Optics,* vol. 18, pp. 1559–1566, 1981.
[8] S. T. Shipley and I. A. Graffman, "ASOS ceilometer measurements of aerosols and mixed layer height in the lower troposphere," *Preprint Volume* of the *Seventh Joint Conference on Applications of Air Pollution Meteorology, American Meteorological Society,* (Boston MA), pp. J228–J229, 1991.
[9] S. T. Shipley *et al.*, "High spectral resolution lidar to measure optical scattering properties of atmospheric aerosols. 1: Theory and instrumentation," *Appl. Opt.*, vol. 22, pp. 3716–3724, 1983.
[10] C. J. Grund and E. W. Eloranta, "University of Wisconsin high spectral resolution lidar," *Opt. Eng.*, vol. 30, pp. 6–12, 1991.
[11] J. D. Spinhirne *et al.*, "Visible and near IR lidar backscatter observations on the GLOBE Pacific survey missions," *Preprint Volume of the Seventh Symposium on Meteorological Observations and Instrumentation, American Meteorological Society,* (Boston MA), pp. J261–J264, 1991.
[12] S. W. Henderson *et al.*, "Eyesafe coherent laser radar system at 2.1 μm using Tm, Ho:YAG Lasers," *Opt. Lett.*, 1991.
[13] E. Raschke *et al.*, "World climate research programme sea-ice and climate," International Council of Scientific Unions and World Meteorological Organization, Rep. WMO/TD-No. 442, 1991.
[14] C. M. R. Platt *et al.*, "An experimental cloud lidar pilot study (ECLIPS)," International Council of Scientific Unions and World Meteorological Organization, Rep. WMO/TD-No. 251, 1988.
[15] D. O. Starr, "A cirrus cloud experiment: Intensive field observations planned for FIRE," *Bull. Amer. Meteor. Soc.*, vol. 67, pp. 119–124, 1987.
[16] R. Reiter and H. Jäger, "Results of 8-year continuous measurements of aerosol profiles in the stratosphere with discussion of the importance of stratospheric aerosols to an estimate of effects on the global climate," Meteorol. Atmos. Phys., vol. 35, pp. 19–48, 1986.
[17] J. A. Reagan *et al.*, "Assessment of extinction to backscatter ratio measurements made at 694.3 nm in Tucson, Arizona," *Aerosol. Sci. Technol.,* vol. 8, pp. 259–275, 1984.
[18] J. D. Spinhirne and W. D. Hart, "Cirrus structure and radiative parameters from airborne lidar and spectral radiometer observations," *Mon. Wea. Rev.,* vol. 118, pp. 2329–2343, 1990.
[19] T. E. DeFoor, "Early lidar observations of the June 1991 Pinatubo eruption plume at Mauna Loa, Hawaii," *Geophys. Res. Letts.,* vol. 19, pp. 150–154, 1992.
[20] B. M. Herman *et al.*, "The effect of atmospheric aerosols on scattered sunlight," *J. Atm. Sci.,* vol. 28, pp. 419–428, 1971.
[21] C. J. Grund, "Measurement of cirrus cloud optical properties by high spectral resolution lidar," PhD. thesis, University of Wisconsin-Madison, 1987.

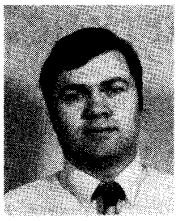

James D. Spinhirne was born in Winslow, IL on March 4, 1948. He received the B.Sc. degree in engineering physics from the University of Illinois in 1970. In 1974 he received the M.S. degree in electrical engineering and in 1977 the Ph.D. degree in atmospheric physics from the University of Arizona. His graduate research was in laser atmospheric studies.

From 1978 to present he has been employed at the NASA-Goddard Space Flight Center in Greenbelt, MD as a scientist in the Goddard Laboratory for Atmospheres with broad interests in remote sensing, instrument development, and atmospheric radiation and climate. As part of his work at Goddard he has been the principle scientist for the NASA ER-2 high altitude aircraft cloud observation experiment. He has been directly responsible for the cloud lidar system, which has operated on the ER-2 since 1983 as the first fully autonomous laser radar remote sensing instrument, and several multichannel cloud radiometers. He has participated in the investigator team for over a dozen large scale atmospheric field experiments including the First ISCCP Regional Experiment for cloud radiation and dynamics and including development and application of a visible and near IR lidar system on the NASA DC-8 for the Global Backscatter Experiment. He was a member of the Laser Atmospheric Sounder and Altimeter definition panel for the Earth Observing System project of the Mission to Planet Earth. He is currently a science team member of the Geoscience Laser Altimeter System spacecraft instrument which is under development for EOS.

Dr. Spinhirne is a member of the American Meteorological Society, OSA, and AGU.